Elasticity and plasticity : foams near jamming

Siemens, A.O.N.

Chapter 2

Introduction

Many everyday materials such as sand, toothpaste, mayonnaise and shaving foam exhibit an intriguing mix of liquid-like and solid-like behaviors, some familiar, some surprising but often poorly understood. These materials all have in common a consistency of disordered collections of macroscopic constituent particles: sand is a dense packing of solid grains (Fig. 2.1 a)), toothpaste is a dense packing of (colloidal) particles in fluid (Fig. 2.1 b)), mayonnaise is an emulsion consisting of a dense packing of (oil) droplets in an immiscible fluid (Fig. 2.1 c)), and shaving foam is a dense packing of gas bubbles in fluid (Fig. 2.1 d)).

Dense is the keyword here – these materials obtain finite rigidity once their constituent particles are brought into contact. Nevertheless, all these materials can be made to flow by the application of relatively small stresses – in fact their utility often stems from precisely this combination of liquid-like and solid-like behavior. By varying thermodynamic (temperature or density) and mechanical (applied stress) variables, one can bring about a transition from a freely flowing to a *jammed* state in these and many other disordered media. For instance an increase in density causes colloidal suspensions to turn glassy. Similarly, flowing foams can be made static by decreasing the applied stress to below the yield stress. In 1998, Liu and Nagel presented a novel way of organizing the physics underlying these phenomena through a jamming diagram (Fig. 2.1e)), and proposed to probe various transitions to rigidity [1].

This Chapter aims at giving a basic introduction to our current understanding of the following two questions: What is the nature of the jammed state? And what is the nature of the jamming transition? We will illustrate the main features of these systems by idealized pictures illustrating our current understanding rather than "real" experimental and numerical

data. For a more elaborate introduction, the reader is referred to two more detailed review papers and references therein [11, 12].

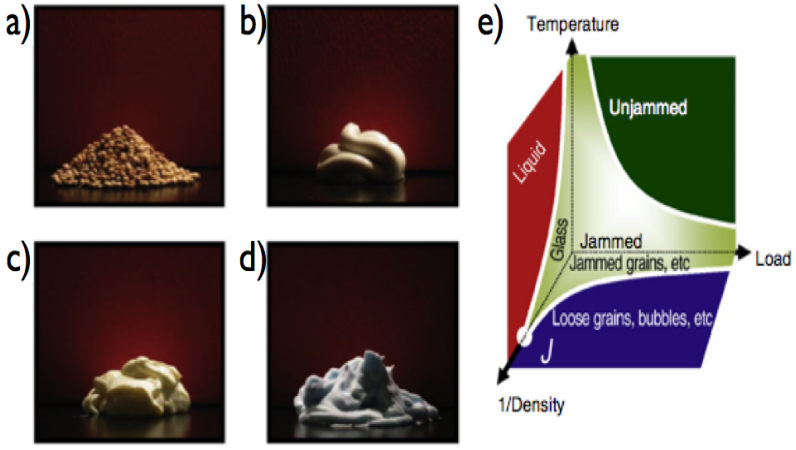

Figure 2.1 – (a-d) Examples of everyday disordered media in a jammed state. a) Granular media. b) Toothpaste. c) Mayonnaise. d) Shaving foam. e) Jamming diagram as proposed by Liu, Nagel and coworkers [1, 13]. The diagram illustrates that many disordered materials are in a jammed state at low temperature, low load and large density, but can yield and become unjammed when these parameters are varied. In this Chapter we will focus on the zero temperature, zero load axis. For frictionless soft spheres, there is a well-defined jamming transition indicated by point "J" on the inverse density axis, which exhibits similarities to an (unusual) critical phase transition.

We will deal only with zero temperature packings of frictionless soft spheres that interact through purely repulsive contact forces. "Soft" in this case means that the individual particles can be deformed under relevant loads – deformations are key. We review the geometrical and mechanical properties of these systems as a function of the distance to jamming.

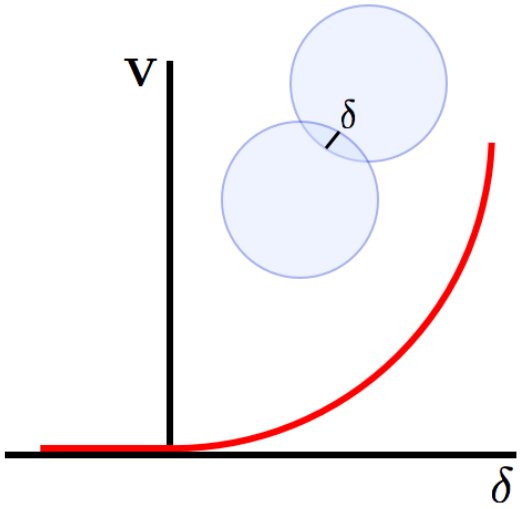

Figure 2.2 – The interaction potential V for pairs of interacting soft frictionless spheres is a simple function of the particles overlap, δ, only.

2.1 Jamming in a Simple Model

Over the last decade, tremendous progress has been made in our understanding of what might be considered the "Ising model" for jamming: static packings of soft, frictionless spheres that act through purely repulsive contact forces. The beauty of such systems is that they allow for a precise study of a jamming transition. In this section we introduce this model, discuss some aspects of its jamming transition and discuss its main parameters.

2.1.1 Model

The most studied and best understood model for jamming consists of soft spherical particles that only interact when in contact, with the interaction forces set by the amount of virtual overlap (similar to deformations for real particles or bubbles) between two particles in contact. Moreover, the contact forces are purely repulsive. No frictional forces, and no attraction is included.

Denoting the undeformed radii of particles in contact as R_i and R_j and the center-to-center distance as r_{ij}, it is convenient to define a dimensionless overlap parameter δ_{ij} as

$$\delta_{ij} := 1 - \frac{r_{ij}}{R_i + R_j} \ , \tag{2.1}$$

so that particles are in contact only if $\delta_{ij} \geq 0$. Since we only will study static properties here, there is no need for specifying a dissipative mechanism.

Power law interaction potentials take on the form (see Fig. 2):

$$\begin{aligned} V_{ij} &= \delta_{ij}^{\alpha} \qquad \delta_{ij} \geq 0 \ , \\ V_{ij} &= 0 \qquad\quad\ \ \delta_{ij} \leq 0 \ . \end{aligned} \tag{2.2}$$

For harmonic interactions, $\alpha = 2$, while Hertzian interactions (the non-linear contact laws for elastic spheres in 3D) correspond to $\alpha = 5/2$. By varying the exponent α the nature and robustness of various scaling laws can be probed.

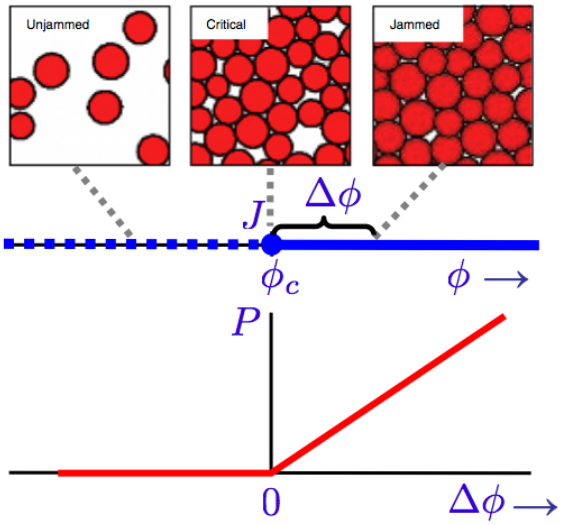

Figure 2.3 – Top: examples of repulsive soft particles below, at and above the jamming transition. The jamming point for frictionless soft spheres is referred to as point J. The packing density ϕ controls the transition here, and the jamming transition occurs at the critical value ϕ_c. The distance to jamming is given by the excess density $\Delta\phi$. Bottom: when the particles have simple harmonic interactions (when they overlap), the pressure grows linearly with excess density.

2.1.2 The Jamming Point

What is the jamming transition for this simple system? The main features are illustrated in Fig. 2.3. As the packing density of the particles, ϕ, is increased, the jamming transition occurs when essentially all particles start to touch but still are at zero pressure – this is called *point J*. Here ϕ_c, the critical packing fraction, is the point at which the particles start touching.

The distance to the jamming point can be measured as $\Delta\phi = \phi - \phi_c$, see Fig. 2.3 [13].

An alternative measure of the distance to jamming is the pressure in the system. If the particles are not in contact, the contact forces between the particles are zero, and so is the pressure. Once particles start to overlap, contact forces arise, and the pressure becomes non-zero, see Fig. 2.3. In fact, one can show that the pressure and the contact forces scale similarly – $P \sim \langle f \rangle$, where brackets denote the average over the system. For the simple interactions used here, and in the absence of gravity, there cannot be a finite force in part of the system, while other parts of the system are at zero pressure. Hence, for finite pressure, the vast majority of particles experience finite contact forces (typically a few percent of the particles are *rattlers*, particles that have only zero contact forces).

Once the pressure is non-zero, the system is jammed. With this we mean that, first, the system has finite elastic moduli, so that applying infinitesimally small forces to the system leads to a proportional and reversible deformation. Second, the system has a finite yielding threshold: if we force the system so much that irreversible deformations arise, the amount of force is *finite* [13].

There are two important things to note: First, for finite systems, the jamming density ϕ_c varies between realizations – this is why one measures the distance to jamming by $\Delta\phi$ and not with ϕ. A disadvantage of using the excess density is that one must first obtain a value for ϕ_c. For simulations this can be done by starting with a jammed system and deflating the particles until the system is not rigid anymore [13]. This step is not necessary when the pressure is a control parameter, since at point J, $P = 0$.

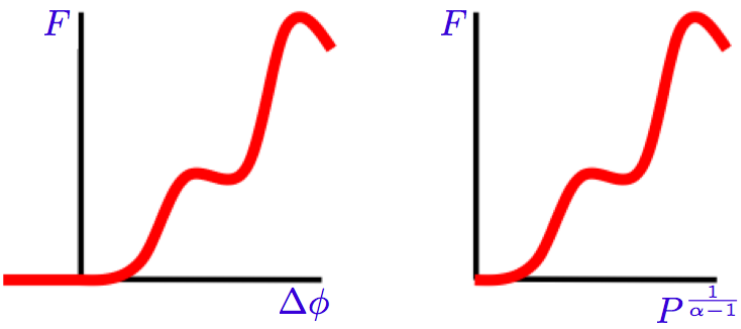

Figure 2.4 – Any function F of the excess packing density $\Delta\phi$ can be translated to a function of the pressure P – for power law interactions of the form Eq. 2.2, $P \sim (\Delta\phi)^{\alpha-1}$.

To relate $\Delta\phi$ and P, we note that the typical particle overlap δ scales as $\Delta\phi$. To relate the pressure and the typical particle overlap, we note that $P \sim f$, and that the force is just $f = -\nabla V_{ij}$. For power law interactions of the form Eq. 2.2 the potential is a function of the overlap, and hence we can relate $\Delta\phi$ and P as follows:

$$P \sim f = \frac{dV_{ij}}{d\delta} \sim \delta^{\alpha-1} \sim (\Delta\phi)^{\alpha-1}. \tag{2.3}$$

As is illustrated in Fig. 2.4, quantities measured as function of $\Delta\phi$ and as function of P can be directly translated.

Secondly, for infinite systems, ϕ_c tends to a well-defined value, directly related to *Random Close Packing* of hard (undeformed) spheres. Random close packing is a notoriously tricky concept, since it is not always clear what random means. An attempt to model RCP based on experimental systems has only recently found some success [14]. In three dimensions, the densest possible packing is the regular FCC packing (similar to how oranges are packed in your grocery store), which reaches a packing density of 74%. What is now the densest random packing? For example, packings consisting of large FCC clusters that are irregularly stacked can attain densities arbitrarily close to the FCC density but still be called random. However, in the absence of any appreciable order, the densest random packings have $\phi_{RCP} \approx 0.64$ (in three dimensions – in two dimensions $\phi_{RCP} \approx 0.84$). Probing the jamming transition with a specific protocol may be seen as defining the RCP density [13]. It is important to note here that monodisperse systems in 2D tend to crystallize easily. To avoid such crystallization, bidisperse or polydisperse systems are often used [4, 5, 15].

2.2 Jammed Materials are Not Ordinary Solids

Superficially, the jamming transition appears similar to a liquid-solid like transition such as freezing. Is the jammed phase simply a solid? In this section we will show that packings at or near jamming are very different from ordinary, *crystalline* solids. We will focus on the elastic and geometric properties of soft spheres near jamming. To highlight the anomalous behavior of jammed solids, we will first explicitly state what we think the simplest prediction for these properties would be. The simple predictions are essentially based on pictures where one ignores the disorder, so called "effective medium" pictures, which work well for ordered materials. One often assumes deformations of the material to be affine, i.e., the local deformations follow trivially from the global.

But such affine / effective medium predictions fail to describe disordered media, and the failure becomes increasingly pronounced when one approaches the jamming transition. Of course, this approach may appear like setting up a straw man, yet we feel it is a useful strategy to stress a surprising aspect of the jamming transition.

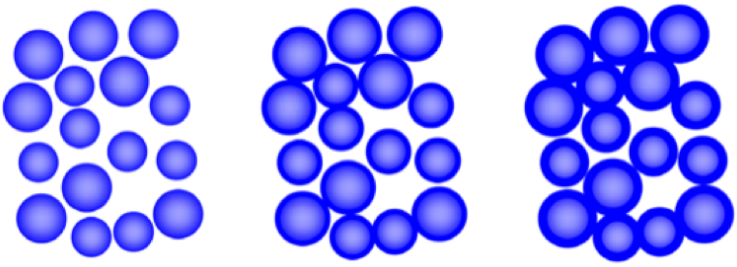

Figure 2.5 – An affine compression of a packing is equivalent to fixing the particles' positions and then inflating their radii.

2.2.1 Contact Number

A key parameter of a packing is its contact number, z, defined as the average number of contacts per particle. To estimate z as function of packing fraction, we start with a low density situation where no particles touch. The simplest estimate of what happens when we compress such a packing is to assume that the local motion of the particles simply follows the globally applied deformation – for compression this is equivalent to inflating all particle radii while keeping their position fixed (Fig. 2.5). More precisely, this uniform compression is an example of an *affine* deformation. A strict definition of affine transformations states that three collinear particles remain collinear and that the ratio of their distances is preserved, and affine transformations are, apart from rotations and translations, composed of uniform shear and compression or dilatation.

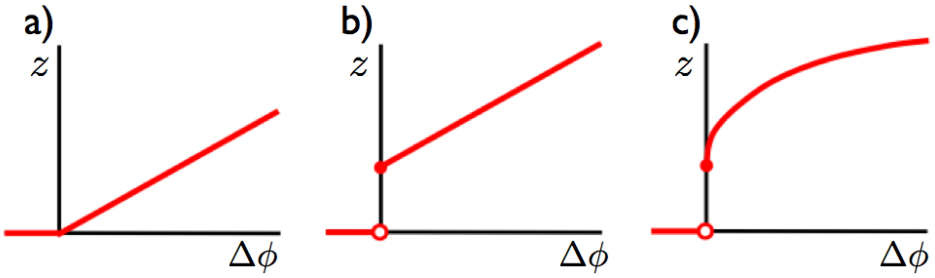

Figure 2.6 – The contact number as a function of the excess packing fraction. a) In the simplest model, the contact number grows linearly with the packing fraction. b) A more realistic model takes into account a minimal contact number (the so-called isostatic value) to begin with, a contact number that at jamming jumps from 0 to $2d$. c) In numerical simulations the contact number grows as the square root of the excess packing fraction above point J.

If the distribution of separations between the initial particles is regular, i.e. all separations occur with similar probability, the contact number grows smoothly from zero under affine compression (Fig. 2.6 a)). This simple model does not balance forces in the packing to make it stable, and as a consequence, the prediction for the growth of the contact number with packing density is far from the numerically observed growth (Fig. 2.6 c)).

Stable packings can only exist once the contact number is above a minimum value, the so-called isostatic value, z_{iso} [16, 17]. Suppose we have N soft frictionless spheres in d dimensions. The contact number equals z. The total amount of contacts in the packing is then $Nz/2$, since each contact is shared by two particles. For a packing to be stable, we require that it should not include floppy modes (which cost zero energy in lowest order, see Fig. 2.7 a)). It can be shown that this is equivalent to demanding that the $Nz/2$ contact forces balance on all particles. For every particle we have d force constraints (force balance in x-direction, y-direction and so forth), so force balance yields Nd constraints on $Nz/2$ force degrees of freedom. One generally expects solutions to such equations only when $z \geq 2d$. The isostatic contact number equals $z_{iso} = 2d$.

At point J, the pressure is zero, so the particles are undeformed. The distance between two particles is therefore exactly the sum of their radii, giving $Nz/2$ constraints for the Nd positional degrees of freedom. The only trivial solutions are when $z \leq 2d$. Combining these two inequalities yields that at jamming, the contact number for frictionless spheres equals precisely $2d$.

We are now able to make another guess at how z should scale with $\Delta\phi$. If we were to incorporate the balance of forces in our model, we would

imagine that at point J, z would jump from 0 to 4 and then grow linearly for $\Delta\phi \geq 0$, as in Fig. 2.6 b). So what happens in simulations?

In 1997, Durian found that the contact number for a 2D system approaches $z = 4$ near jamming and that $z-4$ scales non-trivially as the square root of the excess packing fraction above point J [13, 18], $\Delta z \sim \sqrt{(\Delta\phi)}$, as seen in Fig. 2.6 c). Most surprisingly, subsequent studies found that this relation is independent of the interaction potential and dimension.

Hence, the contact number already shows highly nontrivial behavior: first, it reaches a well-defined value at the jamming point, and secondly, it grows as a nontrivial power law above jamming. Most mechanical properties depend sensitively on z, and so we can already anticipate that the scaling of these will be surprising too.

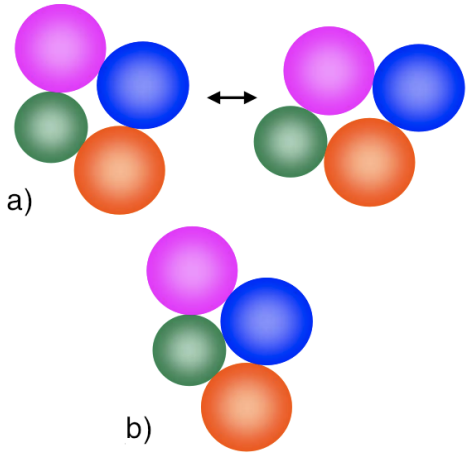

Figure 2.7 – a) For low contact numbers, these packing can be deformed without deforming the particles – this is a (simple) example of a floppy mode. b) For sufficiently large contact numbers, there are no zero energy deformations of this packing possible – apart from trivial translations and rotations. Of course, we could move particles away from one another without energy cost. To make the counting more rigorous, one should consider packings with well-defined boundary conditions.

2.2.2 Elastic Moduli

The elastic moduli of disordered packings show peculiar scaling with distance to the jamming point. When dealing with disordered media, the problem of how to take the disorder into account always arises. Ignoring disorder is an option, but then one can only describe ordered packings. A more subtle approach is provided by the Effective Medium Theory (EMT).

EMT assumes: *(i)* Macroscopic, averaged quantities can be obtained by a simple coarse graining procedure over the individual contacts. *(ii)* Applying a global deformation trivially translates to changes in the local deformation. For example, a 1% strain on the entire sample will deform all the contacts between particles by 1%. This second assumption is the "affine assumption" [19].

Before confronting the predictions from EMT with direct numerical simulations, we have to discuss briefly the elasticity of individual contacts in disordered packings. Under small deformations, a packing of soft, frictionless spheres is equivalent to a spring network, where each contact represents a spring. For a harmonic interaction potential, the spring constant is independent of the force; the spring constant of all contacts has the same value. For anharmonic potentials, such as the Hertzian and Hernian interactions discussed above, this is not true. When we start from an already compressed packing, and thus compressed contacts, and want to quantify the effect of additional small perturbations. The spring constant, k, is then given by

$$k = \frac{d^2V}{d\delta^2}, \tag{2.4}$$

where V is the potential, which typically is a power law function of the compression of the springs. Indeed we find for harmonic interactions ($V \sim \delta^2$), the spring constant is independent of the particles' deformation, and that for general power law interactions ($V \sim \delta^\alpha$), the spring constant scales as $k \sim \delta^{\alpha-2} \sim (\Delta\phi)^{\alpha-2}$.

2.2.2.1 Compression Modulus

The compression modulus (or bulk modulus), K, determines the resistance of a disordered packing against homogenous compression. Under the affine assumption, for a global strain ϵ_{global} applied, this translates directly to the local strain ϵ_{local} felt by all particles. The changes in contact force then scale as $k\epsilon_{\text{local}} \sim k\epsilon_{\text{global}}$, which tells us the elastic modulus is of order k: the elastic moduli follow the typical stiffness of the contacts. Therefore, $K \sim (\Delta\phi)^{\alpha-2}$ [13, 20, 21].

Numerical simulations on disordered packings are consistent with this: the affine assumption works well for compression, although this is a lucky coincidence [21]. Of course the elastic moduli are zero in unjammed packings, and there is, for $\alpha \leq 2$, a discontinuous jump of K in simulations, see Fig. 2.8.

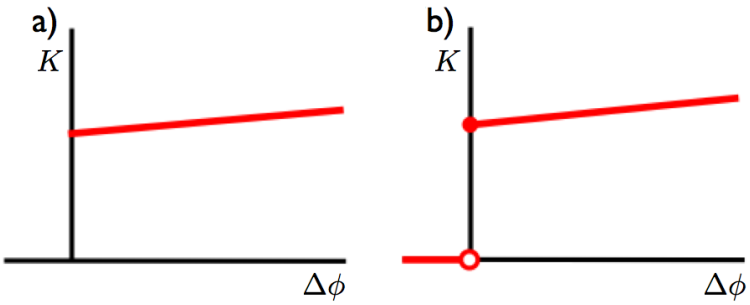

Figure 2.8 – The bulk modulus for packings with harmonic interactions, as a function of the excess packing fraction $\Delta\phi$ in the Effective Medium Theory picture a) and for simulations b). In both cases, slight variations in the modulus with $\Delta\phi$ are expected due to an increase of the density of contacts with compression, but this does not influence the scaling behavior near $\Delta\phi = 0$.

2.2.2.2 Shear Modulus

The shear modulus, G, determines the resistance of a disordered packing against pure shear. Following arguments similar to those for the compression case, EMT predicts that the shear modulus scales as $G \sim (\Delta\phi)^{\alpha-2}$ [13, 19, 20, 21].

Numerical simulations on disordered packings show a different scaling, however: the actual shear modulus scales as $G \sim (\Delta\phi)^{\alpha-3/2}$ [13, 19, 20, 21], see Fig. 2.9.

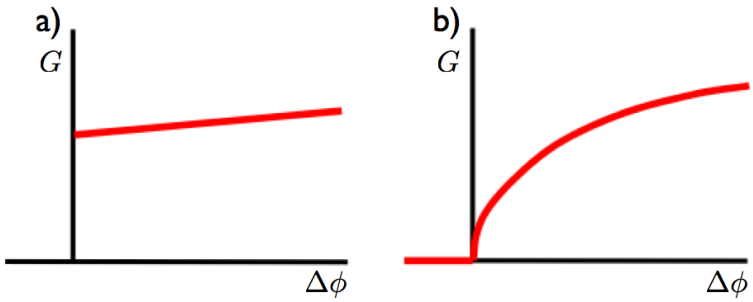

Figure 2.9 – The shear modulus for packings with harmonic interactions, as a function of the excess packing fraction $\Delta\phi$ in the Effective Medium Theory picture a) and for simulations b). For shear, the affine assumption breaks down spectacularly.

Hence, close to jamming, the system is much softer to shear deformations than to compressive deformations, and the ratio of G/K goes to zero,

independent of interaction potential. In fact, making use of the scaling of $\Delta z \sim \sqrt{\Delta\phi}$ one can write this ratio as $G/K \sim \Delta z$.

2.3 Beyond Effective Medium Theory

In the previous section we have seen that the contact number and the elastic properties signal the unique nature of materials near the jamming transition. In this section we briefly sketch *why* these materials behave so differently. We in particular stress the breakdown of the affine assumption.

2.3.1 Nonaffine Deformations

The anomalous scaling of the elastic moduli is related to the nonaffine nature of the deformations of weakly jammed packings, although the precise connection is rather subtle. We will discuss our current understanding below.

An instructive way to illustrate the role of these nonaffine deformations is first, to force the particle displacements to be affine and then let them relax, while measuring the changes in the elastic energy (governed by the elastic moduli) in both cases.

O'Hern and coworkers found that the elastic moduli associated with the affine deformations scale precisely as predicted by effective medium theory. However, the forced system can lower its elastic energy by additional nonaffine motion of the particles. These nonaffine deformations are particularly effective for shear deformations, as they are found to change the scaling of the shear modulus [13].

It is tempting to conclude that the nonaffinity is stronger for shear deformations than for compressive deformations. However, subsequent studies have found that for both shear and compression the nonaffine deformations are large, and in fact diverge near jamming [20]. To characterize the local deformations, note that changes in elastic energy depend on the relative motion of pairs of contacting particles as

$$\Delta E = \frac{1}{2}\sum_{i,j} k_{ij}\left(u_{\parallel,ij}^2 - \frac{\delta_{ij}}{\alpha - 1} u_{\perp,ij}^2 \right) , \tag{2.5}$$

here $u_\parallel$ and $u_\perp$ are relative motions of particles parallel and perpendicular to each other, respectively (see Fig. 2.10). Note that u does not refer to flow, but to small, quasi-static displacements in response to external forcing. The $u_\perp$ arises from applying Pythagoras theorem, and using Eq. 2.4 to related k and δ, see [12].

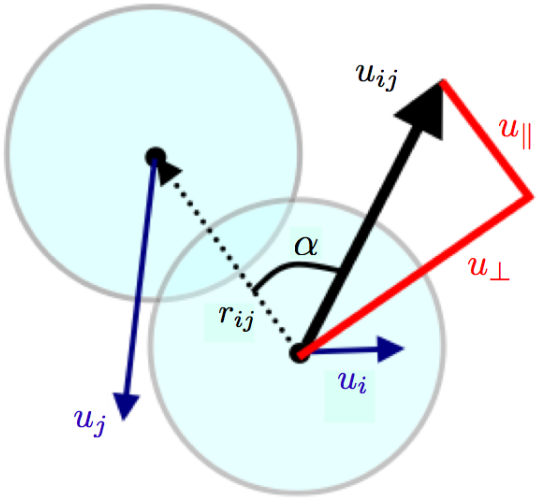

Figure 2.10 – Definition of the relative motion u_{ij} of two particles that each move by u_i and u_j respectively, and the corresponding $u_{\parallel}$ and $u_{\perp}$.

We now need a parameter to capture the degree of nonaffinity, something that dictates how the system on a local scale responds to an imposed shear or compression as compared to an expected affine response. The probability distribution, $P(\alpha)$, does just this. Ellenbroek and coworkers introduced the displacement angle α_{ij} [20]. Here α_{ij} denotes the angle between $\mathbf{u}_{ij}$ and $\mathbf{r}_{ij}$ (see Fig. 2.10), or,

$$\tan \alpha_{ij} = \frac{u_{\perp,ij}}{u_{\parallel,ij}} \ . \tag{2.6}$$

Affine compression corresponds to a uniform shrinking of the bond vector between two particles, i.e. $u_{\perp,ij} = 0$ and $u_{||,ij} = -\epsilon r_{ij} \leq 0$, where ϵ is the magnitude of the applied strain on the system. In this scenario, $P(\alpha)$ exhibits a delta-function peak at $\alpha = \pi$. For affine shear, the effect depends on the bond vectors orientation, and for isotropic random packings, $P(\alpha)$ is flat.

In numerical simulations one finds that for large pressures, $P(\alpha)$ is not too different from the affine prediction, but that closer to point J, $P(\alpha)$ develops a substantial peak around $\pi/2$. These correspond to contacts where $u_{\perp} \gg u_{\parallel}$ – in other words, to contacts, where the particles in essence slide past each other. Surprisingly, this peak develops and appears to diverge both for shear and compressive deformations [21, 22].

In addition one can investigate the scaling of $u_{\parallel}$ and $u_{\perp}$ as well. The typical values of $u_{\parallel}$ under a deformation are directly connected to the cor-

responding elastic modulus: for compression, $u_{\|}$ is essentially independent of the distance to jamming ($u_{\|} \sim \epsilon$), while for shear, $u_{\|} \sim \epsilon\ \Delta\phi^{1/4}$, where ϵ is the magnitude of the strain [21, 22].

The scaling for $u_{\perp}$, the amount by which particles in contact slide past each other, is more subtle. Numerically, one observes that for shear deformations, $u_{\perp} \sim \epsilon\ \delta^{-1/4}$. The two terms $\propto u_{||}$ and $\propto u_{\perp}$ become comparable here, and the amount of sideways sliding under a shear deformation diverges near jamming [20, 21, 22]. For compression there is no simple scaling. Knowing that $\Delta z \sim \sqrt{\Delta\phi}$, the above expressions for $u_{\|}$ and $u_{\perp}$, and guessing that in this case the two terms in Eq. 2.6 would balance, one might have expected $u_{\perp} \sim \epsilon\ \delta^{-1/2}$. However, the data suggests a weaker divergence, close to $\Delta\phi^{-0.3}$. Nevertheless, both under shear and compression, the sliding, sideways motion of contacting particles dominates and *diverges* near jamming.

The preceding findings illustrate the strange nature of linear response close to the jamming transition.

2.4 Experimental Review

We have seen that soft frictionless spheres near the jamming transition exhibit a wealth of nontrivial and unexpected behavior, that the response is strongly nonaffine and the elastic moduli are anomalous. However, the approach we have taken above is strictly theoretical and it is helpful to get a good overview of elasticity experiments on jamming to the present date as well.

Experiments on 3D foam and emulsions were performed in the 1980's, focusing on cone-plate and Taylor-Couette geometries [23, 24, 25, 26, 27, 28, 29, 30]. First estimates of the scaling of the shear modulus with respect to the packing fraction were obtained by Princen and Kiss [28] using polydisperse oil-in-water emulsions. This work was followed in the 1990's by Mason et al. [30], who suggested the variation versus the packing fraction for monodisperse emulsions. They found a linear dependence: $G \sim \phi(\phi - \phi_c)$, where $\phi_c \approx 0.64$ is the critical packing fraction in three-dimensional, monodisperse packings. Mason et al. found that the osmotic pressure scaled similar to the shear modulus with ϕ, which means that the bulk modulus, being the derivative of the pressure, has to differ significantly from the shear modulus at ϕ_c, although the data is noisy. They also did not observe that the ratio G/K goes to zero at the jamming point. Mason did, however, also stress the importance of the nonaffine motion in their emulsions, if they were sheared close to the critical point. He hypothesized

that these motions arose from localized relaxations of the droplet positions. This was later confirmed by O'Hern et al. in simulations [13].

In all these studies, however, a real relation between bulk rheology and the behavior at the single particle level was never established. What actually happens on the bubble-bubble scale under a continuous shear strain, for example? For small applied strain, the bubbles are deformed minutely, yet still want to restore their equilibrium surface area. They respond elastically, the way a solid would [31]. If the strain is increased further, the foam relaxes through bubble rearrangements [23]. With a large enough strain the system starts to flow irreversibly and there are continuous rearrangements [24, 32]. This type of behavior is of course dependent on how far from the critical point the system is. In dry foams, far from ϕ_c, [33, 34, 35] found that rearrangements in the form of so-called T1 events, where two nearest-neighbor particles become next-nearest neighbors, (discussed in greater detail in Chapter 5) negate the build-up of stress. No experimental studies have focused on plasticity in wet foams close to ϕ_c as of yet.

The structure of these elastic systems was also carefully examined close to the jamming point. Imaging of 3D packings of foams and emulsions to look at static structures needs some sophisticated imaging techniques to peer through the opaque samples, such as DWS [36], x-ray tomography [37] and confocal microscopy [14, 38, 39]. In 2D, Bolton [40] found that the critical packing fraction for a system of disordered discs was $\phi_c = 0.842$ and that two-dimensional, disordered systems [41] do not exhibit a linear increase of G near ϕ_c in 2D, contrary to results for 3D systems used by Mason, although the osmotic pressure did increase quadratically near ϕ_c.

The study of flow in bubble packings was studied extensively by [4, 5], where the packing fraction is controlled precisely. In this work, Katgert et al. showed how great control of a two-dimensional foam can yield interesting behavior of the shear modulus. By controlling the packing fraction, they were able to show the square-root scaling of the packing fraction with the contact number with correct prefactors, as well as velocity profiles of bubbles in a packing under shear.

A different approach to what has been seen so far was taken by Cheng [15], who used the swelling of confined tapioca particles to go through the jamming transition to observe the nonaffine behavior there. In this seminal work, Cheng found the classic signature of the jamming transition by observing the tell-tale first (and second) peak in the pair-correlation function. Furthermore, by looking at the displacement fields, he found that a static length scale in the system reached the system size at ϕ_c. Further

work probing the jamming transition, using hydrogel particles, which are polymers that swell when introduced to salty water, is being performed by the van Hecke group, as well as the Behringer group.